Title	Cyclic viscoplasticity testing and modelling of a service-aged P91 steel
Author(s)	Farragher, Tadhg P.; Leen, Sean B.
Publication Date	2014-04-16
Publication Information	Hyde, CJ, Sun, W, Hyde, TH, Rousse, JP, Farragher, T, O Dowd, N.P., Leen, SB, (2014) 'Cyclic viscoplasticity testing and modelling of a service-aged P91 steel'. Journal Of Pressure Vessel Technology, 136 (044501).
Publisher	American Society of Mechanical Engineers
Link to publisher's version	10.1115/1.4026865
Item record	http://hdl.handle.net/10379/5453
DOI	http://dx.doi.org/10.1115/1.4026865

Journal of Pressure Vessel Technology - PVT-12-1136

CYCLIC VISCO-PLASTICITY TESTING AND MODELLING OF A SERVICE-AGED P91 STEEL

C. J. Hyde
Department of Mechanical, Materials and Manufacturing Engineering, The University Of Nottingham, University Park, Nottingham, NG7 2RD, UK

W. Sun
Department of Mechanical, Materials and Manufacturing Engineering, The University Of Nottingham, University Park, Nottingham, NG7 2RD, UK

T. H. Hyde
Department of Mechanical, Materials and Manufacturing Engineering, The University Of Nottingham, University Park, Nottingham, NG7 2RD, UK

J. P. Rouse
Department of Mechanical, Materials and Manufacturing Engineering, The University Of Nottingham, University Park, Nottingham, NG7 2RD, UK

T. Farragher
Mechanical and Biomedical Engineering, College of Engineering and Informatics, NUI Galway, Galway, Ireland

Noel P O'Dowd
Materials & Surface Science Institute, University of Limerick, Limerick, Ireland

S. B. Leen
Mechanical and Biomedical Engineering, College of Engineering and Informatics, NUI Galway, Galway, Ireland

ABSTRACT

A service-aged P91 steel was used to perform an experimental programme of cyclic mechanical testing in the temperature range of 400°C to 600°C, under isothermal conditions, using both saw-tooth and dwell (inclusion of a constant strain dwell period at the maximum (tensile) strain within the cycle) waveforms. The results of this testing were used to identify the material constants for a modified Chaboche, unified visco-plasticity model, which can deal with rate-dependant cyclic effects, such as combined isotropic and kinematic hardening, and time-dependent effects, such as creep, associated with visco-plasticity. The model has been modified in order that the two-stage (non-linear primary and linear secondary) softening which occurs within the cyclic response of the service-aged P91 material is accounted for and accurately predicted. The characterisation of the cyclic visco-plasticity behaviour of the service-aged P91 material at 500°C is presented and compared to experimental stress-strain loops, cyclic softening and creep relaxation, obtained from the cyclic isothermal tests.

INTRODUCTION

Many components in power generation plant, chemical plant, aeroengines and superplastic forming dies etc, are subjected to high levels of mechanical loading under harsh environments such as high temperatures in order to achieve high levels of output/efficiency from the systems of which they form a part. The materials undergoing operation under these conditions are often working under an inelastic state where the temperatures are high enough for creep to play a significant role in the evolution of deformation and damage of the material over time. Therefore, an understanding of the material behaviour at high temperature is very important for the design and lifetime prediction of components made from such materials.

Unified material models represent a robust method of modelling the behaviour of materials for high temperature cyclic loading. The Chaboche unified viscoplasticity model, for example, includes both non-linear isotropic hardening and kinematic hardening processes, as well as viscous (creep) effects. This model was first proposed by Chaboche and Rousselier [1, 2].

The present paper is concerned with the application of the Chaboche unified viscoplasticity model, which has been developed in uniaxial form in Matlab, to a service-aged P91 steel. Strain rate and strain range have a significant effect on the behavior of the material which is captured within the model. However, within this paper, uniaxial test specimens have been cyclically tested, at 500C, under fully reversed (R_ε = -1), isothermal conditions at only a strain rate and strain range of 0.1%/s and ±0.5%, respectively. The service-aged P91 material has been used purely as a demonstrative material for the experimental and modeling results. Therefore no comparison to virgin P91 material and the affect that the previous loading history of the service-aged P91 has on the cyclic behaviour and life of the material has been made.

Two types of waveform have been considered, namely the 'saw-tooth' and 'dwell' type waveforms (see Figure 1), where the 'dwell' waveform includes a two minute constant strain dwell period at the maximum strain within each cycle, during which creep behaviour is observed in the form of relaxation. This service-aged P91 material consistently exhibits a two-stage cyclic softening behaviour made up of a primary, non-linear region and a secondary linear region, as shown in Figure 2. For the present work it is only up to the end of the secondary softening region of the cyclic behaviour which has been considered, the tertiary (failure) behaviour shown in Figure 2 is not considered.

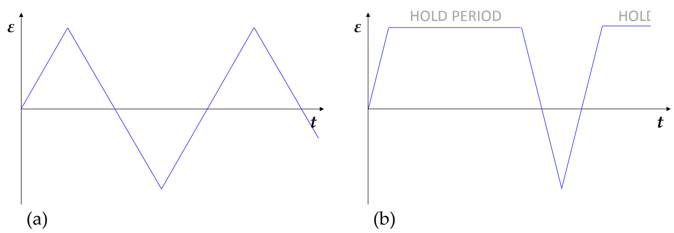

Figure 1. Schematic representation of the (a) saw-tooth and (b) dwell waveforms.

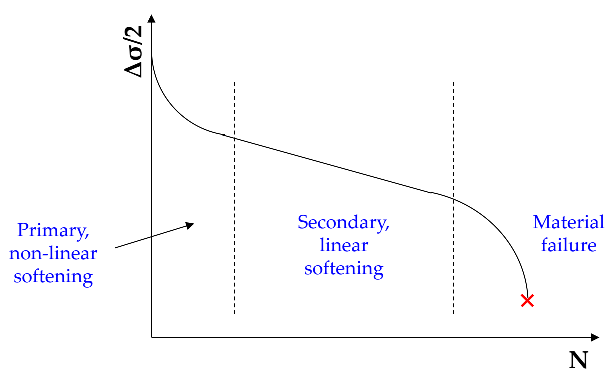

Figure 2, Schematic representation of the cyclic primary (non-linear) and the secondary (linear) softening as well as the material failure behaviour.

The model has therefore been adapted in order to account for secondary cyclic softening behaviour. Isothermal material data has been used in order to obtain initial material constants for the adapted model using similar methods previously described [3, 4]. A least squares optimisation algorithm (also developed in Matlab) has then been applied to the material constants in order to provide a further improvement to the general fit of the model to experimental data. This optimisation procedure is required due to some assumptions which must be made in order to obtain the initial values of the material constants from experimental data. The initially obtained material constants, obtained from experimental data, were used as the starting point in this optimisation process and sensible upper and lower boundaries for each material constant were applied.

Model predictions, using both the initial and optimised material constants, are compared to experimental data. Data to model comparisons are shown for stress-strain loops at various times during the life of the test specimen, the corresponding creep relaxation curves where appropriate (i.e. for the 'dwell' type waveform) and the cyclic softening behaviour.

DEFINITION OF THE MATERIAL MODEL

The cyclic (uniaxial) material behaviour of the service-aged P91 material has been represented by the Chaboche unified viscoplasticity model. The uniaxial form of the model is as follows:

$$\dot{\varepsilon}_p = \left\langle \frac{f}{Z} \right\rangle^n sgn(\sigma - \chi) \tag{1}$$

$$sgn(x) = \begin{cases} 1 & x > 0 \\ 0 & x = 0 \\ -1 & x < 0 \end{cases} \text{ and } \langle x \rangle = \begin{cases} x & x > 0 \\ 0 & x \le 0 \end{cases}$$

where Z and n are material constants, ε_p is the plastic strain, f represents the model yield criterion (see equation (2)), σ is the stress within the material (see equation (3)) and χ is the kinematic hardening parameter (see equations (4) and (5)).

$$f = |\sigma - \chi| - R - k \tag{2}$$

$$\sigma = \chi + (R + k + \sigma_v) sgn(\sigma - \chi) = E(\varepsilon - \varepsilon_p) \tag{3}$$

The elastic domain is defined by $f \le 0$ and the inelastic domain by $f > 0$, R represents the isotropic hardening parameter as described by equation (6), k is the initial yield stress, σ_v is the viscous stress as described by equation (8), E is Young's modulus and ε is the total strain.

$$\dot{\chi}_i = C_i (a_i \dot{\varepsilon}_p - \chi_i \dot{p}) \tag{4}$$

$$\chi = \sum_{i=1}^{j} \chi \tag{5}$$

$$\dot{R} = b(Q - R)\dot{p} + H\dot{p} \tag{6}$$

where for the present work, j has been chosen to be 2. b, Q, C_i and a_i are material constants and p is the accumulative plastic strain, given by:-

$$\dot{p} = |\dot{\varepsilon}_p| \tag{7}$$

It is the second term ($H\dot{p}$) with equation (6) which account for the secondary linear softening behaviour (see Figure 3). The physical meanings of kinematic hardening and isotropic hardening in terms of the influence they have on the yield surface are shown in Figure 3. Figure 3 shows the types of hardening in the three-dimensional (principal) stress space. When the stress state within the material causes the yield surface to be reached, kinematic hardening, implemented by equations (4) and (5), is represented as the movement of the yield surface, as illustrated in part (a) of Figure 3. Isotropic hardening, implemented by equation (6), represents the growth of the yield surface, as shown in part (b) of Figure 3.

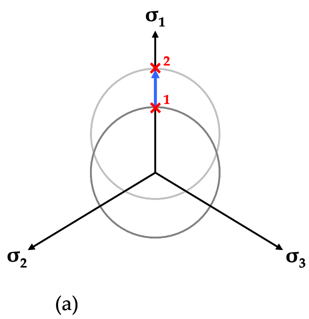

Figure 3. Schematic representations of (a) kinematic and (b) isotropic cyclic hardening behaviour.

Viscous (creep) effects are also accounted for within the model, in the form of the Norton [5] creep law, as follows:

$$\sigma_v = Z\dot{p}^{1/n} \tag{8}$$

The basic equation within the model, the viscoplastic flow rule, is shown by equation (1). All other equations shown (equations (2) to (8)), show that all of the other model variables, such as those used for calculating both types of hardening and viscous stress are dependent on the value of accumulated plastic strain, p, calculated in turn, as shown by equation (7), from the plastic strain (ε_p) values obtained from this viscoplastic flow rule. The above model has been implemented, in uniaxial form, within Matlab, a high level programming language.

MODEL PREDICTIONS

In order for model predictions to be produced, 11 material constants must first be identified using experimental data. Methods for obtaining the initial estimations of the material constants have been described by Zhan [6] and Gong et al [3]. These material constants are then subjected to a simultaneous parameter optimisation routine where each constant has user defined upper and lower boundaries. Such an optimisation procedure must be used in order to provide further accuracy to the material constants due to the assumptions which must be made in the initial identification of the material constants from experimental data. This optimisation is regarded as a means to 'tighten-up' the material constants and it is ensured that the procedure is not simply a mathematical search for any set of material constant that fit the experimental by the application of the upper and lower boundaries for each material constant ensuring that the 'ballpark' initial figures are not deviated too far from during the optimisation.

The need for an optimisation procedure stems from the assumptions made when estimating initial values for the material constants, namely:

- Initially, all hardening is assumed to be isotropic to determine the related hardening parameters.
- When estimating kinematic hardening constants, it is assumed (for the integration of the related differential equations) that the viscous stress remains constant.
- It is assumed that the contribution of certain back stress components is significant only in certain time periods.
- Commonly, initial estimates of the visco-plastic material constants are approximated by trial and error or taken from literature.

The Levenburg-Marquardt algorithm (a gradient based optimisation procedure similar to the well-known Gauss-Newton method) has been implemented for this optimisation problem through the MATLAB function LSQNONLIN. In this function, the Chaboche model ODEs are solved using MATLAB's ODE45 function (using an adaptive step $4^{th}/5^{th}$ order Runge-Kutta method). The data from a 'saw-tooth' waveform test is applied to the optimisation procedure using two objective functions (corresponding to stress-strain loops and cyclic softening) and the data from a 'dwell' waveform test is applied using three objective functions (corresponding to stress-strain loops, cyclic softening and the creep relaxation which occurs during the constant strain dwell periods). Table 1 to Table 4 show the initially obtained constants for the service aged P91 at 500°C for the saw-tooth and dwell waveforms (see Figure 1) and the optimised equivalents, respectively.

Table 1. Initial estimates of the model constants for the saw-tooth waveform.

E **(GPa)**	***k*** **(MPa)**	***b***	***Q*** **(MPa)**	***H*** **(MPa)**	a_1 **(MPa)**	C_1	a_2 **(MPa)**	C_2	***Z*** **(MPa.s$^{1/n}$)**	***n***
172.64	28.02	0.78	-77.45	-2.06	121.86	1676.78	141.37	401.45	320.11	12.33

Table 2. Initial estimates of the model constants for the 'dwell' waveform.

E **(GPa)**	***k*** **(MPa)**	***b***	***Q*** **(MPa)**	***H*** **(MPa)**	a_1 **(MPa)**	C_1	a_2 **(MPa)**	C_2	***Z*** **(MPa.s$^{1/n}$)**	***n***
171.57	14	0.98	-101.88	-1.63	109.11	8528.2	156.66	545.34	320.11	12.33

Table 3. Optimised model constants for the saw-tooth waveform.

E	***k***	***b***	***Q***	***H***	a_1	C_1	a_2	C_2	***Z***	***n***

(GPa)	(MPa)		(MPa)	(MPa)	(MPa)		(MPa)		(MPa.s$^{1/n}$)	
156.31	7.83e-004	2.54	-59.05	-1.84	45.04	4607.47	109.72	379.69	807.55	6.55

Table 4. Optimised model constants for the 'dwell' waveform.

E (GPa)	k (MPa)	b	Q (MPa)	H (MPa)	a_1 (MPa)	C_1	a_2 (MPa)	C_2	Z (MPa.s$^{1/n}$)	n
173.82	12.66	1.01	-101.36	-1.63	125.22	6654.84	127.61	341.48	318.18	12.34

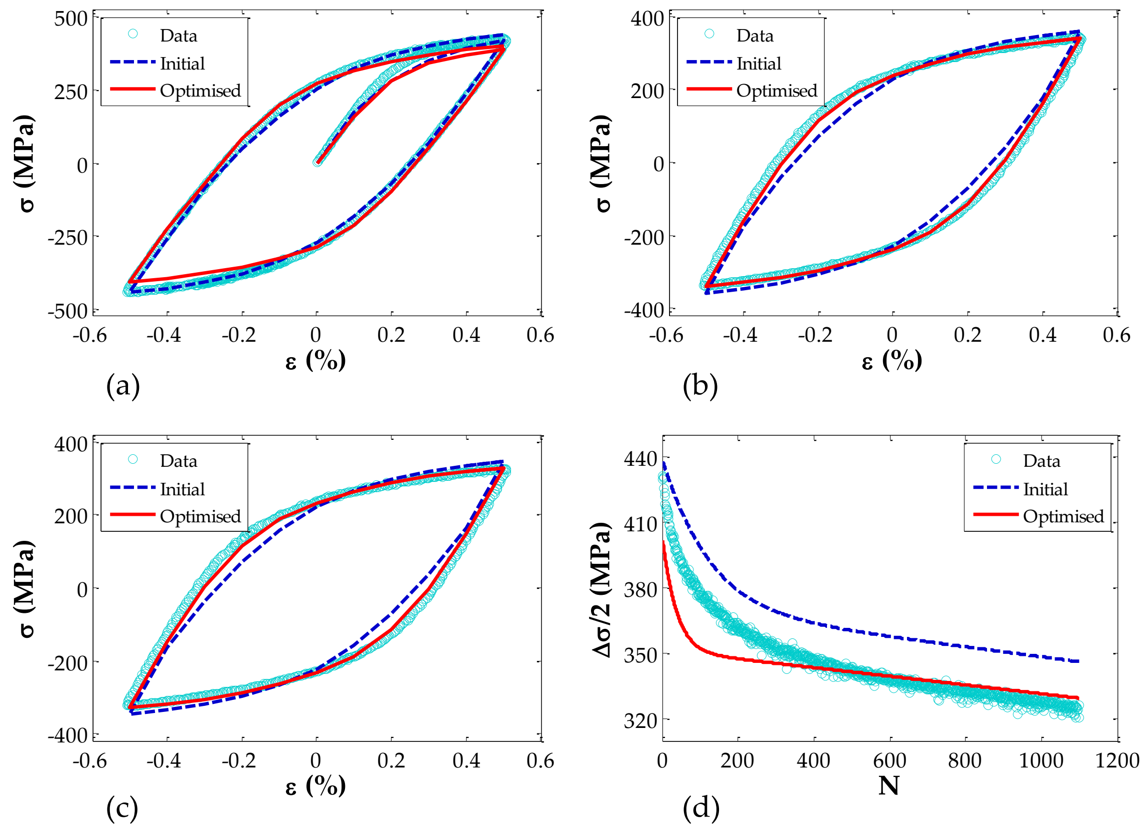

Figure 4. Model predictions to experimental data comparisons for the saw-tooth waveform (a) 1st σ-ε loop, (b) 575th σ-ε loop, (c) 1100th σ-ε loop and (d) cyclic softening behaviour.

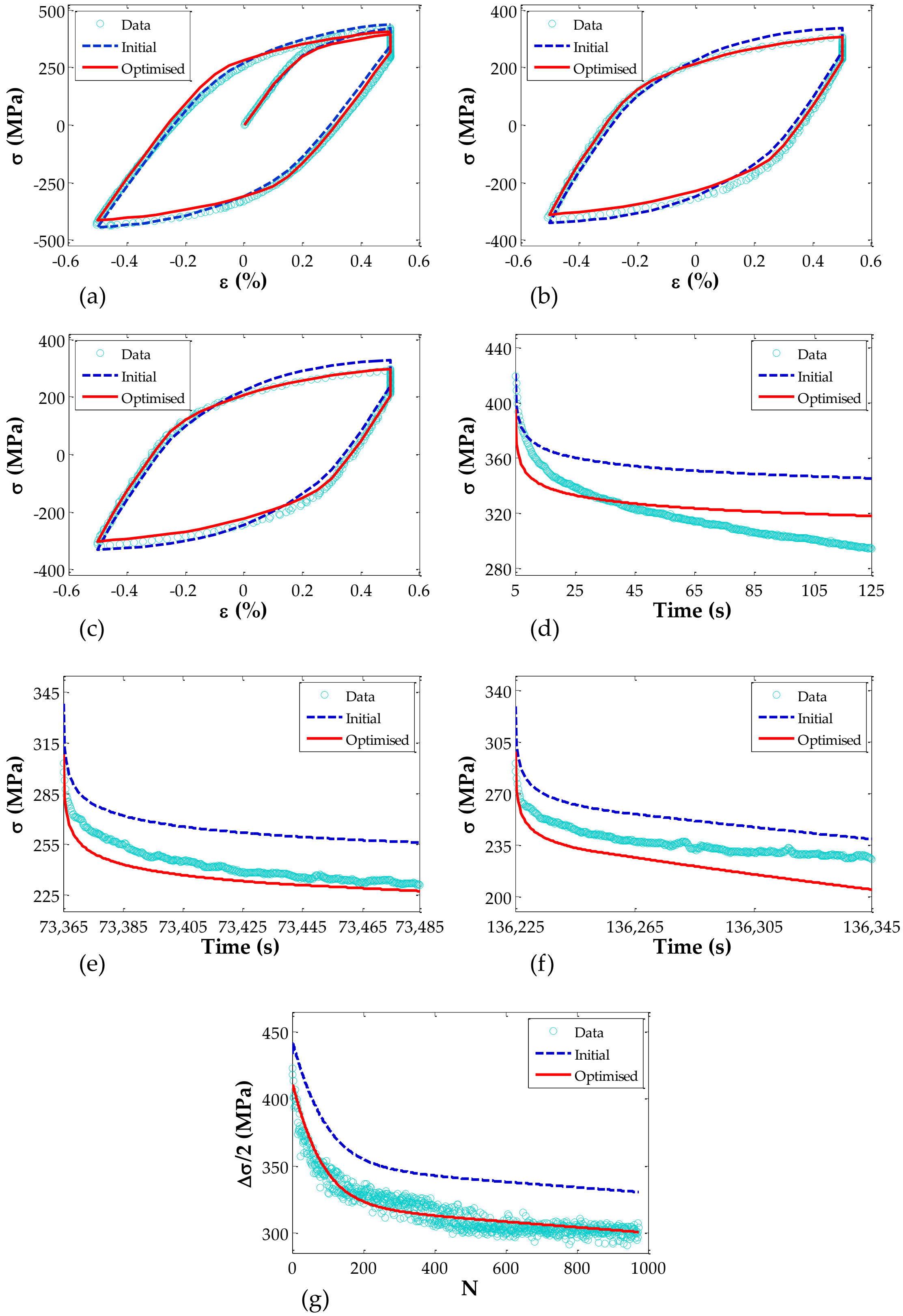

Figure 5. Model predictions to experimental data comparisons for the 'dwell' waveform (a) 1st σ-ε loop, (b) 525th σ-ε loop, (c) 975th σ-ε loop, (d) 1st relaxation period, (e) 525th relaxation period, (f) 975th relaxation period and (g) cyclic softening behaviour.

DISCUSSION

A unified, viscoplasticity material model developed in uniaxial form within Matlab, has been successfully applied to the experimental data for a service-aged P91 at 500°C. The methods for obtaining an initial set of material constants for this model as well as an optimisation procedure used for improving these material constants have been used as described in previous publications by Gong et al [3].

Two types of waveform have been presented, namely saw-tooth and ‘dwell’ waveforms (see Figure 1), where the dwell waveform includes a constant strain ‘dwell’ period at the maximum cycle strain. For the saw-tooth profile the considered output data is the stress-strain loops and the cyclic softening curve. For the dwell profile, however, a third data type is considered, namely, the creep relaxation which occurs during the constant strain dwell periods. The data types form the objective functions of the optimisation procedures. For the saw-tooth profile data, therefore a two objective function optimisation procedure was used and for a ‘dwell’ profile data, a three objective optimisation procedure was used. The inclusion of the third objective function puts a higher weighting on the accuracy of the creep constants and therefore improves the accuracy in predicting the viscous effect, which becomes particularly important under high temperature conditions.

Typical model predictions for both types of waveform, using both the initial and optimised constants have been presented and compared to experimental data, showing both the improvement made by use of the optimisation procedure as well as the extremely good fit of the optimised model predictions to the experimental data. Different material constants were determined by the optimisation procedure for the same aged P91 material when different loading conditions were considered (namely the saw-tooth and dwell-type waveforms). This may be in part due to the lack of a creep dominant region in the saw-tooth type waveform (meaning viscous parameters have less data to be optimized against). For the successful implementation of the Chaboche model in component analysis problems a single set of material constants must be determined at a given temperature, strain rate etc. It is the intent of the authors, within future work, to produce an optimisation procedure which considers both saw-tooth and dwell-type waveforms and generate a single set of material constants per temperature.

From the experimental data presented (as well as for the temperatures tested but not presented), it can be seen (Figure 4 and Figure 5) that the material consistently cyclically softens in both the primary (non-linear) and secondary (linear) regions. This is reflected in the model by negative values of Q and H (see equation (6)), respectively. For an initially hardening material, however, the value of Q would be positive and for a material which then entered a secondary, linear hardening region, H would be positive. Alternatively, for a material which gives a period of cyclic saturation after the initial (non-linear) hardening/softening region, H would equal 0.

ACKNOWLEDGMENTS

The authors would like to thank Mr Stephen Scully of ESB Energy International, Cork, Ireland, for supplying the service-aged material. Thanks are also given to Tom Buss at the University of Nottingham for his assistance with the experimental work and to Noel O’Dowd for his assistance in the project. This publication has emanated from research conducted with the financial support of Science Foundation Ireland under Grant Number SFI/10/IN.1/I3015.

REFERENCES

[1] Chaboche, J. L. and Rousselier, G., "On the Plastic and Viscoplastic Constitutive equations - Part 1: Rules Developed With Internal Variable Concept", Journal of Pressure Vessel Technology 105 (1983), 153-158.

[2] Chaboche, J. L. and Rousselier, G., "On the Plastic and Viscoplastic Constitutive equations - Part 2: Application of Internal Variable Concepts to the 316 Stainless Steel", Journal of Pressure Vessel Technology 105 (1983), 159-164.

[3] Gong, Y. P., Hyde, C. J., Sun, W. and Hyde, T. H., "Determination of material properties in the Chaboche unified viscoplasticity model", Proceedings of the Institution of Mechanical Engineers, Part L: Journal of Materials: Design and Applications 224 (2010), no. 1, 19-29.

[4] Hyde, C. J., Sun, W. and Leen, S. B., "Cyclic thermo-mechanical material modelling and testing of 316 stainless steel", European Creep Collaborative Committee, publisher, Zurich, Switzerland, 2009, pp. 55 - 69.

[5] Norton, F. H., "The creep of steel at high temperature, McGraw Hill, New York, 1929.

[6] Zhan, Z., “A Study of Creep-Fatigue Interaction in a New Nickel-based Superalloy”, University of Portsmouth, *PhD Thesis*, 2004.